

Lunar Micro Rover Design for Exploration through Virtual Reality Tele-operation

Nathan Britton, Kazuya Yoshida, John Walker, Keiji Nagatani, Graeme Taylor, and Loïc Dauphin

Abstract A micro rover, code-named Moonraker, was developed to demonstrate the feasibility of 10kg-class lunar rover missions. Requirements were established based on the Google Lunar X-Prize mission guidelines in order to effectively evaluate the prototype. A 4-wheel skid steer configuration was determined to be effective to reduce mass, maximize regolith traversability, and fit within realistic restrictions on the rover's envelope by utilizing the top corners of the volume.

A static, hyperbolic mirror-based omnidirectional camera was selected in order to provide full 360° views around the rover, eliminating the need for a pan/tilt mechanism and motors. A front mounted, motorless MEMS laser scanner was selected for similar mass reduction qualities. A virtual reality interface is used to allow one operator to intuitively change focus between various narrow targets of interest within the wide set of fused data available from these sensors.

Lab tests were conducted on the mobility system, as well as field tests at three locations in Japan and Mauna Kea. Moonraker was successfully teleoperated to travel over 900m up and down a peak with slopes of up to 15°. These tests demonstrate the rover's capability to traverse across lunar regolith and gather sufficient data for effective situational awareness and near real-time tele-operation.

1 Introduction

A case study for a low cost lunar exploration mission is presented in this section to establish a general set of requirements for a lunar micro rover. The case study is based on the Google Lunar X-Prize (GLXP) and the goals of GLXP team Hakuto.

Britton, Nathan
Tohoku University, Sendai, Miyagi, JAPAN e-mail: nathan@astro.mech.tohoku.ac.jp

Yoshida, Kazuya
Tohoku University, Sendai, Miyagi, JAPAN e-mail: yoshida@astro.mech.tohoku.ac.jp

1.1 Google Lunar X-Prize

The GLXP is a privately funded competition to land a rover on the surface of the Moon, with prize money of \$30 million USD available to privately funded teams who accomplish certain pre-determined goals, primarily to traverse 500m across the lunar surface and transmit HD video and photographs to earth. The GLXP requirements are considered essential minimum capabilities for the design of a micro-rover and for performance assessments.

Tohoku University's Space Robotics Lab (SRL) is in partnership with Hakuto, an official team contending for the GLXP. Hakuto has exploration goals in addition to the minimum GLXP requirements, detailed in Sec. 1.2, and provides the SRL with requirements based on the methods for launch, trans-lunar injection, and landing.

1.2 Landing Site and Exploration Target

In 2009, Haruyama et al. discovered evidence of collapsed lava tube skylights from JAXA's SELENE images of the surface of the moon[2]. Since then, many potential skylights have been discovered from various satellite imagery. The landing target is one of these potential skylights in the region known as Lacus Mortis, or "Lake of Death", south of Mare Frigoris in the northern, Earth-facing hemisphere of the Moon.

Team Hakuto plans to land within 500m of the skylight, which can be found at 44.95°N, 25.61°E, just south of a rille known as Rimae Bürg. Based on NASA's Lunar Reconnaissance Orbiter (LRO) images, the skylight is just under 400m in diameter, with the south-eastern edge of the pit collapsed, forming a natural ramp from the lunar surface to the cavern floor (Fig. 1).

Data from the Lunar Orbiter Laser Altimeter (LOLA) instrument of LRO also exist for this region[3]. The data is too sparse to develop a full digital elevation map, but does suggest a minimum average slope angle of 13°(Fig. 1 and Table 1). Tests with lunar regolith simulants have found that the angle of repose (maximum stable angle of a granular material) of lunar mare regolith can be up to 45-50° in Earth gravity and as high as 58° in lunar gravity[1].

The slope of the skylight ramp is likely varied, but *cannot be estimated more precisely than between 13° and 58°*; from safe to highly hazardous. There is insufficient data to determine a distribution within this range, therefore the feasibility of an unassisted descent must be decided on-site. In order to maximize the probability for and reduce the risks of a potential extended mission into the skylight, designing for stability during steep-slope traversal is a high priority.

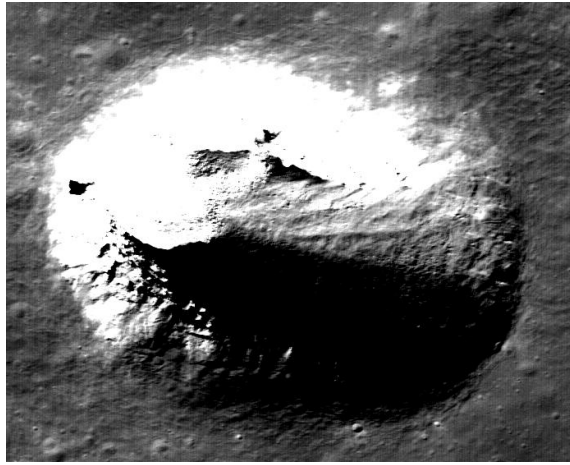


Fig. 1 The target skylight near Rimae Bürg, with the collapsed eastern wall clearly visible [4]. LOLA data (Table 1) indicate that the altitude at the eastern edge is -2042m, and a point in the center of the skylight, 150m from the edge, is -2077m altitude. 35m of depth across 150m indicates that the minimum average angle of the slope can be estimated at 13.13° .

#	Longitude	Latitude	Altitude	Estimated Location
1	25.6222222	44.9595561	-2043.09	Vicinity East of the skylight
2	25.6222346	44.957638	-2042.38	Vicinity East of the skylight
3	25.6226786	44.9585525	-2042.14	Vicinity East of the skylight
4	25.616147	44.9562664	-2040.64	Southern edge of the skylight
5	25.6161021	44.9601059	-2077.34	<i>Center of the skylight, 150m from #2</i>
6	25.6165264	44.962933	-2055.96	Northern edge of the skylight

Table 1 Lunar Orbiter Laser Altimeter (LOLA) measurements in the vicinity of the lava tube entrance[3]. One reading from the center of the pit suggests a minimum depth of 35m.

1.3 Communication Architecture

Hakuto plans to use the lander hardware to support a fixed communication relay station to the Earth. By eliminating the need for the micro-rover to establish a direct connection to the Earth, a greater portion of the mass budget can be allotted to mobility and imaging subsystems and other payloads. This architecture has benefits which apply to potential missions beyond the scope of the GLXP. In any situation where a permanent base station is nearby the micro-rover's tasked operation zone, this architecture is effective for reducing mass.

For the prototype and field tests discussed in this paper, a laptop was used to emulate the function of a stationary lander, and 802.11 wireless networks used for communication. A lower frequency radio communication system with lower bandwidth is planned for the flight model, but not included in this paper. For this particular case study, should the traversal into the skylight be successful, fully autonomous exploration of the skylight is necessary due to the communication blackout; however full automation experiments are also not considered in this report.

1.4 Requirements

- Mass limit: **10kg**
- Stowed volume envelope: **50cm(length) x 40cm(width) x 30cm (height)**
- Use of a nearby base station as relay to Earth
- Travel at least *500m* across the surface
- Climb as steep an incline of regolith as possible (*minimum 13°*)
- Ability to take *self portraits* and display relevant logos
- Full 360 degree HD panoramic stills: *0.3mrad/pixel*, 8bit color



Fig. 2 Moonraker traversing over a mountain at Izu Oshima (Sec. 3).

2 Testbed Moonraker

Based on the case study mission and requirements, a micro rover prototype code-named Moonraker was constructed for Earth-based testing and validation. In order to meet the strict size constraints, redundancy is reduced, with greater focus on reliability to mitigate risk. Non-essential actuation points were removed where possible to minimize mass, power consumption, and the total number of failure modes. The final mass and power budgets can be seen in Table 2. The resulting system is unique among similar micro-rover missions, such as the 1997 Mars Pathfinder rover component Sojourner, particularly due to the large wheel-size to system-size ratio.

Moonraker uses an omnacam, giving full 360° by 80° views of the surrounding environment. A MEMS-based laser range finder (LRF) is equipped on the front, to measure accurate 3D positions of any imminent obstacles. These data, along with an IMU, are fused together in a 3D environment for viewing with a virtual reality headset. The mobility system consists of four 20cm wheels, for a large wheel-size to body-size ratio. Each wheel is independently controlled by 12W motors; maneuvers are conducted through skid steering. The wheels are stowed above the rover body during transit to maximize grouser length allowance.

As indicated in Table 2, the thermal subsystem and solar power generation designs were unimplemented in the terrestrial prototype discussed in this report. Aluminum solar panel mockups, identical in surface area to the flight system design, are used to properly obstruct the environment around the wheels as in a real lunar mission (Fig.2).

Subsystem	Target Mass	Actual Mass		Nominal Power
Mobility	25%	24.6%	2462g	30W
Power	20%	18.9%*	1890g*	
Structure+Thermal	20%	20.3%*	2027g*	
Sensors	10%	9.7%	965g	5W
Avionics+Comms	5%	3.6%	363g	8W
Payload for Sale	5%	8.9%	893g*	
Margin/Cables	15%	14.9%	1493g	
Total	100%	(81%)	10000g*(8107g)	43W

Table 2 Moonraker mass and power budgets. The mass of Moonraker during tests was 8107g.
*indicates estimations based on unimplemented designs.

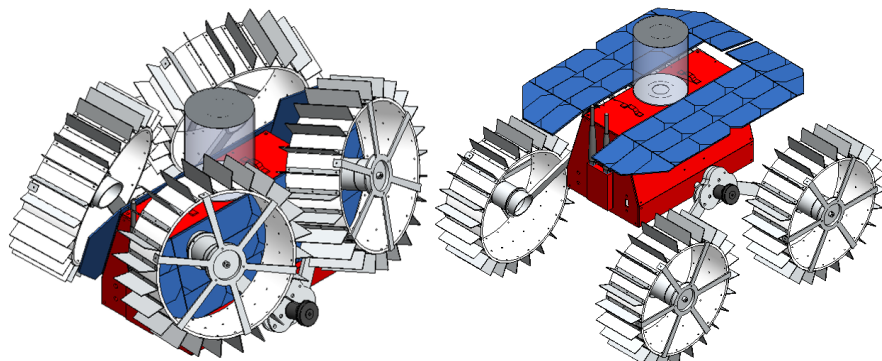


Fig. 3 Moonraker, shown with 25mm grousers, stowed (left) vs deployed (right).

2.1 Sensors

2.1.1 Mirror Omni-Camera

In order to meet the requirements of the case study mission, Moonraker must be equipped with the sensors necessary to construct a full 360° panoramic image, and view itself. A standard camera equipped on a pan/tilt mechanism would be capable of meeting these requirements, but the additional mass necessary for such a mechanism is a challenge to accommodate within a 1kg total sensor mass budget (Table 2). The potential for motor failure also introduces risk that redundancy may be necessary to mitigate. In order to circumvent these challenges, wide FOV camera options were evaluated and a hyperbolic mirror omniscamera was selected as the primary sensor. Using a static camera pointed vertically towards a hyperbolic mirror, the omniscamera system is able to construct 360° panoramic images in single frames.

Using a calibration model developed by Scaramuzza[6], each pixel on the image plane (bottom of Fig.4) can be projected onto a sphere to represent a ray in 3D space through the focus of the hyperbola, as shown in Fig.6. This model is useful for displaying and evaluating the characteristics of the environment, as the spatial relationship between pixels is known. This allows for undistorted views as seen in Fig.5. With a 70mm diameter mirror and 10 megapixel camera, the average visual acuity is estimated to approach 0.3 mrad per pixel.

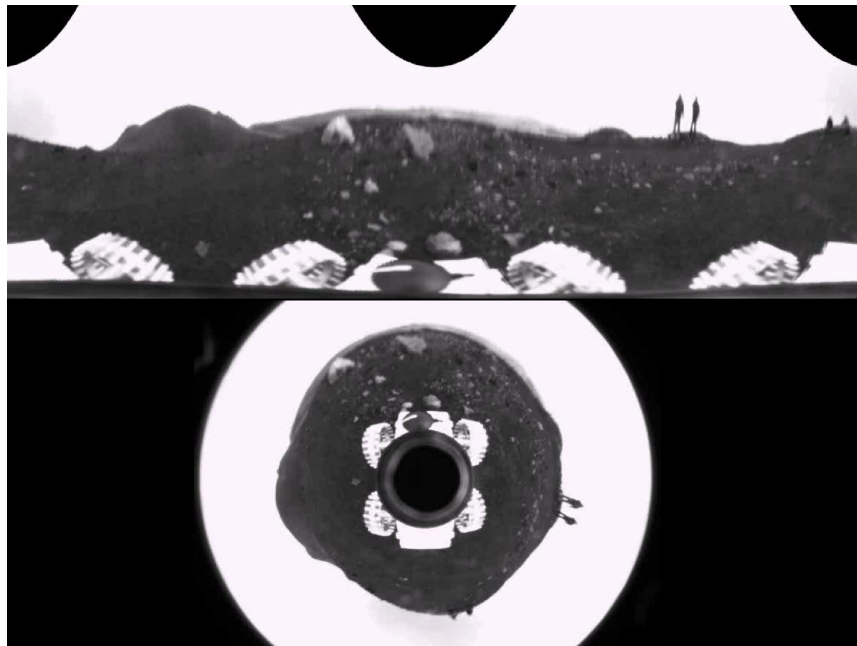


Fig. 4 Omnicamera raw image (bottom) and corresponding panoramic projection (top).

2.1.2 MEMS Laser Range Finder

Although the omnicamera system enables collection of data on the surrounding environment over a wide area, it must be placed on top of the rover to achieve this. This limits visibility in the immediate vicinity in front of the rover, especially where the rover body obstructs the view of the ground. An additional sensor for detecting imminent obstacles and determining their exact position relative to the wheels is therefore highly desirable; a LRF is capable of satisfying these needs.

A MEMS-based LRF is able to achieve a 3D scan over a more narrow field of view than traditional LRF units, but is able to do so without using motors or large moving parts. A small MEMS mirror is precisely controlled to scan an area in front of the sensor, using less power and keeping all moving parts in a small, isolated chamber inside the sensor. The sensor selected for Moonraker (FX8, from Nippon Signal) is able to scan 6000 points over a 60° by 50° region four times per second. The range is specified as 5m, but effective range during field tests rarely exceeded 3m. Although limited for applications requiring full 3D data on the entire surrounding environment, this is sufficient for the requirements of Moonraker.

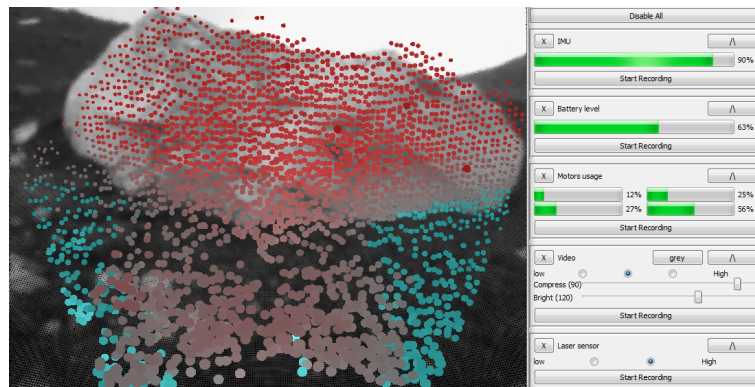


Fig. 5 Technical specialist's graphical interface, with a snapshot of the mission specialist's view of fused sensor data (left) and telemetry with controls for various subsystems(right).

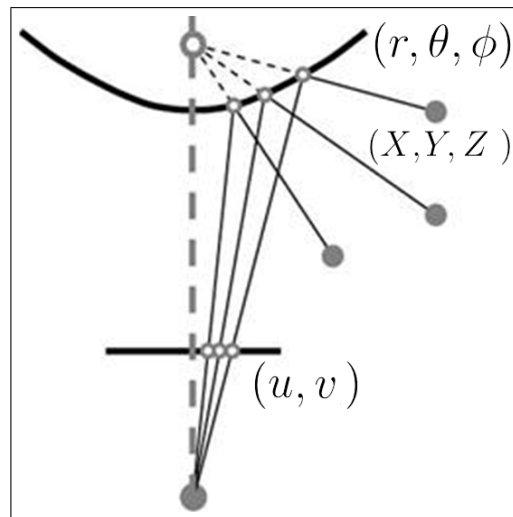
2.2 Teleoperation Interface

Two-person teams under a shared-roles model, with a task breakdown between one mission/payload specialist and one technical specialist, have been found to be highly effective for field robotics teleoperation[5]. Moonraker's teleoperation software interface is designed to reduce potential bottlenecks to understanding and acting on available information quickly.

The mission specialist software implements a virtual reality (VR) interface to Moonraker's sensor data. This allows the operator to easily focus on and intuitively change focus between various narrow targets of interest within a set of wide and otherwise cumbersome data. Without this interface, distortion prevents an accurate understanding of the spatial relationships between obstacles, and navigating the large panoramic image or raw circular data becomes the primary operational challenge.

The technical specialist uses a more traditional mouse-based graphical interface in parallel to view telemetry and control subsystem settings. This support interface is rendered in a window on the same field-laptop (Figure 5), and displays the status of each subsystem. The status of the IMU, remaining battery power, torques and power used by the motors, and the signal strength of the connection with the rover, can be seen. The resolution of both the camera and the LRF, as well as the camera color settings, brightness settings, and compression rate can be controlled. A snapshot of what the mission specialist is doing is available to facilitate effective communication between the operators.

Fig. 6 The pixels on an image plane (u, v) are projected, through the hyperbolic mirror above it, into rays through 3D space (r, θ, ϕ). These rays can be used as unit vectors (X, Y, Z) to compose a virtual semi-sphere for displaying undistorted images as viewed from the focus of the hyperbola, at the center of the sphere. (image source: Scaramuzza[6])



2.2.1 Virtual Reality (Sensor Fusion)

The data from all three sensors (camera, laser, IMU) are fused to provide the VR interface display. The camera system streams compressed video of the panoramic images to the operator computer. These panoramas are undistorted into a spherical projection (Fig.6), and adjusted to match the orientation of the rover from IMU data. Using an open source 3D engine (Ogre3D), the projection is rendered around the position of two cameras.

Frames of pointcloud data from the LRF are synchronized with the camera frames and orientation and are displayed in alignment to give precise distance information about potential obstacles in front of the rover. The HMD used (Oculus Rift) implements stereoscopy, requiring one rendering per eye, which gives the VR operator a natural sense of depth when viewing the pointcloud. The operator can also see any obstacle's position relative to the rover, its wheels and any other feature of interest in view of the camera.



Fig. 7 Mission specialist's graphical interface, with a rendered view of fused camera and LRF data for each eye. A joystick is used to control the mobility system.

2.3 Mobility

2.3.1 Four Wheels

Tracks are known to have advantages over wheels for clearing rough terrain and maximizing contact area with soil, but are also heavier than wheels[9]. Tracks are also less reliable than wheels, due to a susceptibility to failure from jamming, which is difficult or impossible to repair in an exploration mission[7]. Wheels were therefore selected as the mobility system for Moonraker.

More wheels are generally considered to result in higher performance, due to the additional contact points with the surface[10]. A primary advantage of the popular 6-wheel configuration is from rocker-bogie suspension, which facilitates agile traversal over rocky and uneven terrain. This advantage, however, does not apply to the primary mobility challenge of slippage on steep soft regolith slopes of the target lunar mare environment. The two primary wheel parameters that effect slippage on loose soil are *wheel diameter* and *grouser length*.

The envelope length of 50cm (Sec. 1.4) is the primary constraint to wheel size. With a 10cm gap between wheels, in a 6-wheel configuration the space available for wheel and grousers together is 10cm diameter; in a 4-wheel configuration, the diameter doubles to 20cm. Despite its popularity, for mass/volume-limited missions in loose soil environments, *the 6-wheel rocker-bogie design is a waste of valuable wheel diameter potential*, and results in higher risk for slippage in loose soil.

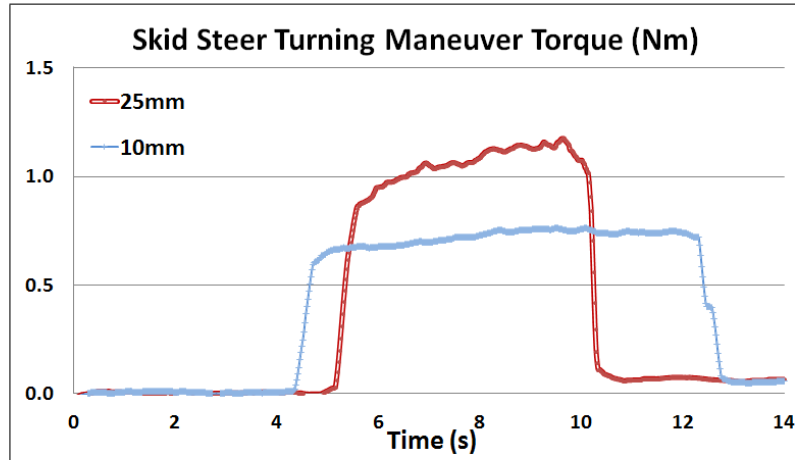


Fig. 8 The average torque per wheel required to perform a 90° spot-turning maneuver. The area under the 10mm curve is 8% larger than the taller 25mm curve.

2.3.2 Grouser Length, Steering and Laboratory Experiment

Increasing the diameter of a wheel and the length of its grousers will improve linear traveling performance over loose soil by decreasing slip. Grouser length has a greater impact on slip than diameter, to the extent that lengthening grousers at the expense of diameter still improves performance[8]. This improved performance directly impacts traversability up steep slopes - a primary requirement for Moonraker. The maximum possible grouser length is therefore desirable for linear travel, however the impact of grouser length on steering is not as well known.

Steering can either be performed precisely by spinning the wheels about the axis perpendicular to the ground with additional motors, or by skid steer, where the difference between the rotational speed of the left and right motors causes rotational slip. Although less precise, skid steering is simpler and more mass efficient. However, the reliance of skid steering on slip and the additional power required to overcome resistance against the soil was expected to reduce traveling efficiency. Experiments were conducted in an indoor laboratory environment to determine the impact of grouser length on skid steering spot-turn maneuvers (turning in place).

Moonraker was equipped with 20cm wheels and comparisons were made between the performance of 10mm grousers and 25mm grousers on operations conducted in a sandbox of Toyura sand, measured with an Osprey motion capture system. The linear slip ratio was calculated to quantify the benefit of the longer grousers for linear performance. The torques of the wheels were also measured during 90° spot-turning maneuvers at a constant speed of 2.9rpms to quantify the difference in skid steering torques. Longer grousers were expected to require more torque, but the extent was not known.

With 10mm grousers, slip began at 8° and by 16° became severe (Fig.9). With 25mm grousers, no measurable slip occurred even at 16°. This dramatic difference in the slip ratio confirms previous research with 2-wheel rovers and, in isolation from steering concerns, result in a preference for 25mm grousers on Moonraker.

Based on the linear performance results, higher requisite torques and expended energy for turning operations was anticipated. As shown in Fig.8, although the torques required for a spot-turning operation with 25mm grousers reach up to 60% higher than with 10mm grousers, the turning operations were in fact completed in almost half the time. *This increases, rather than decreases, the efficiency of spot-turning operations by 8%.*

Our proposed explanation for the unexpected result is that the sand-flow against the wheel during a spot-turn rotational slip approaches a direction parallel to the grousers. The grousers' push against the sand moves the rover, causing a yaw rotation. Longer grousers create greater resistance against the sand in the direction of wheel rotation, but if the rover is not moving forward during the turn, the grousers do not create greater resistance in the direction of the rover's yaw. This allows longer grousers to maneuver the rover more quickly while sand flows between grousers with little resistance. Further testing is required to prove this hypothesis.

2.3.3 Suspension and Wheel Deployment

Using a rocker suspension system ensures that each of the wheels remain in contact with an uneven surface, and when traversing over small rocks. With a vertical envelope restriction of 30cm, the clearance between the rover body and the ground is restricted, which limits traversability over obstacles. In the initial iteration of the Moonraker design, almost 50% of the volume in the 50x40x30cm envelope was empty. It was found that stowing wheels above the rover body, for deployment post-landing, dramatically increased the utilization of the limited envelope.

Placing the stowed wheels diagonally to fill the corners of the volume gives the largest improvement in space available to the wheels. This allowed for an increase in wheel-grouser diameter from 20cm to 25cm, the clearance over the ground from 9cm to 15cm, the wheel width from 4cm to 8cm, and the lateral distance between left and right-side wheels of the rover from 40cm to 50cm. These improvements, which increase stability and traveling performance on slopes, are otherwise not possible with the strict volume limitations.

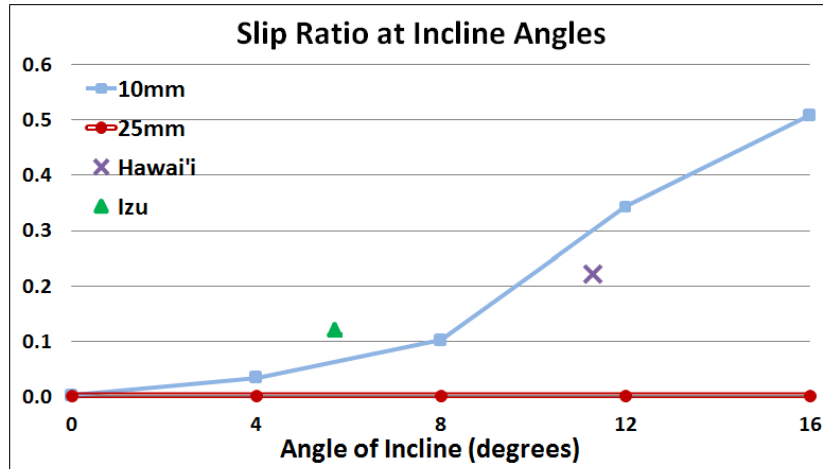


Fig. 9 Slip ratios from lab tests of 10mm and 25mm grousers, compared with field tests(Sec.3).

3 Field Tests

Field tests of Moonraker were conducted on Mt. Aso in Kyushu, Japan (2011), Mt. Mihara at Izu Oshima, Japan (2012), and Mauna Kea, Hawai'i (2013). Each of the test sites provided a range of environments from very soft, loose volcanic ash to rocky pumice, on and near slopes of mountains and volcanic craters. This type of environment is the closest available, on Earth, to what can be expected on the lunar surface. In each test Moonraker was equipped with 10mm grousers and successfully traveled over 500m towards points of interest. Issues in mobility and teleoperation efficiency were identified in each case, informing iterative improvements.

In Kyushu, scattered pumice over loose sand and ash was found at Sunasenri near the Mt. Aso crater. A 600m course was successfully run across the southern edge of the crater. With 6W motors, Moonraker was unable to traverse over small rock obstacles when the incline reached 10° and failed to reach the top of the crater. Motors were subsequently upgraded to 12W for a 5x increase in torque (up to 7Nm/motor).

Izu Oshima provides an environment covered in pumice from coarse sand to rocks. A 900m course up to the peak of Mt. Kushigata from the south and down the north was completed, with an average ascent incline of 5.7° , and a maximum of 15° . The average slip ratio over the course of the ascent was 0.12, as shown in Fig.9, which is slightly higher than the prediction of laboratory tests for soft sand.

In Hawai'i, a 600m course was successfully completed over a sandy area in Hale-wahine Valley on the southern slope of Mauna Kea. A 20° slope of soft dark volcanic ash, with similar mechanical properties to lunar regolith simulant, was found on the north side of the valley. Due a slip ratio approaching 1, direct traversal up the slope was not possible, but by progressing in alternating lateral trajectories, roughly 45° from direct ascent, it was possible to climb 30m (Fig.10). Over a 100m path, at an average incline of 11° , the slip ratio was 0.22 (Fig.9).

This field testing helped to develop the interface, which evolved from simple command line to video and gamepad control to the interface described in Sec. 2.2. Difficulty in control with communication delay have informed the next step in interface development. The next techniques to be implemented in field testing are mapping, semi-autonomy and global coordinate commands.

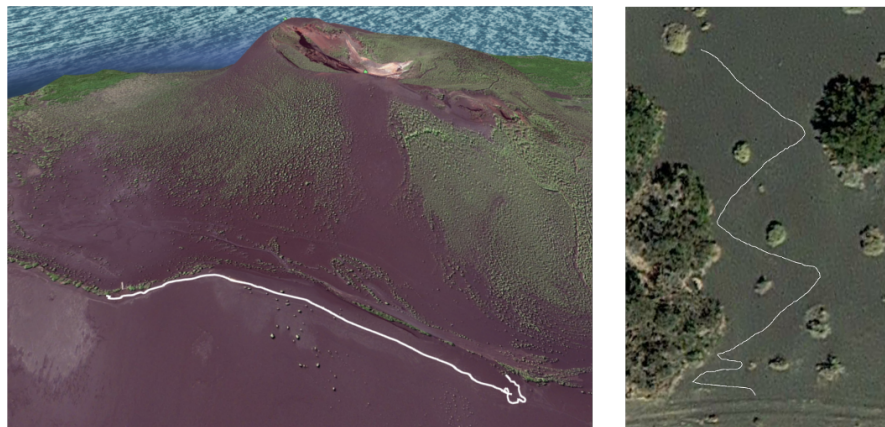


Fig. 10 900m path of a field test over Mt. Kushigata, near Mt. Mihara on Izu Oshima Island, Japan (left). 100m path up a 20° slope of soft volcanic ash performed on Mauna Kea, Hawai'i (right).

4 Conclusion

Micro rovers in the 10kg-class are an attractive option for performing an exploration mission at low cost. Although the reduction in size can limit capability, with careful design, a micro rover can still provide rich data on the explored environment while still being able to provide extensive mobility over across varied terrain.

A micro rover testbed, code-named Moonraker, was designed based on requirements for a specific lunar mission to investigate a lunar skylight. Static sensors which require no moving parts, such as an omnacameras and a MEMS laser range finder allow for a lightweight but effective solution to extensively image the environment and collect sufficient data for full situational awareness. The wide coverage area of the sensors make a virtual reality interface an effective part of a shared-roles teleoperation model, where one operator can intuitively change focus between various narrow targets of interest within a wide set of available data.

A 4-wheel skid steering mobility system demonstrates the potential for high traveling performance on loose soil for micro rovers, if wheel size is not sacrificed to keep the system small. In limited-volume conditions, wheel size can be maximized by utilizing the corner space of the envelope above the rover body. Laboratory experiments were conducted to validate the efficiency of the 4-wheel skid steering maneuvers and found that longer grousers make spot-turn maneuvers more efficient and dramatically improve traversability on inclines of loose soil.

Field tests conducted with Moonraker validate the design by demonstrating successful completion of the case study mission goals. Slip ratio results from the field were found to deviate only marginally from laboratory tests. These real world field tests helped to highlight shortcomings in mobility and software interface, leading to opportunities for effective iterative improvements.

References

1. FRITZ, I. C. Repose behavior of lunar simulants. NASA SEED Program Report, Carthage College, Department of Physics and Astronomy, 2010.
2. HARUYAMA, J., HIOKI, K., AND M., S. Possible lunar lava tube skylight observed by selene cameras. *Geophysical Research Letters* 36, 21 (2009), 1–5.
3. LUNAR ORBITAL LASER ALTIMETER. LOLA RDR Data Products Between 44.957° N, 25.616° E and 44.963° N, and 25.623° E. Washington University, PDS Geosciences Node, 2011.
4. LUNAR RECONNAISSANCE ORBITER CAMERA. LROC Observation M126759036L. Arizona State University, 2010.
5. MURPHY, R. R., AND BURKE, JENNFER, L. From remote tool to shared roles: Human-robot interaction in teleoperation for remote presence applications. *IEEE Robotics & Automation Magazine* 15, 4 (December 2008), 39–49.
6. SCARAMUZZA, D. *Omnidirectional Vision: From Calibration to Robot Motion Estimation*. PhD thesis, ETH ZURICH, 2008.
7. SEENI, A., SCHÄFER, B., AND HIRZINGER, G. Robot mobility systems for planetary surface exploration - state-of-the-art and future outlook: A literature survey. In *Aerospace Technologies Advancements*, T. T. Arif, Ed. InTech, 2010, ch. 10, pp. 189–209. ISBN: 978-953-7619-96-1.
8. SUTOH, M. *Traveling Performance Analysis of Lunar/Planetary Robots on Loose Soil*. PhD thesis, Tohoku University, 2013.
9. WAKABAYASHI, S., SATO, H., AND NISHIDA, S. Design and mobility evaluation of tracked lunar vehicle. *Journal of Terramechanics Volume 46*, 3 (2009), 105–114.
10. ZHANG, P., DENG, Z., HU, M., AND GAO, H. Mobility performance analysis of lunar rover based on terramechanics. In *Advanced Intelligent Mechatronics* (2008), IEEE/ASME International Conference, IEEE. Available via IEEE Xplore.